

An IMEX scheme combined with Richardson extrapolation methods for some reaction-diffusion equations

István Faragó^{1,2,*}, Ferenc Izsák^{1,†}, Tamás Szabó^{3,4,‡}

¹ Department of Applied Analysis and Computational Mathematics
Eötvös Loránd University
H-1117, Budapest, Pázmány P. s. 1/c. Hungary

² HAS-ELTE Reserch Group "Numerical Analysis and Large Networks"
H-1117, Budapest, Pázmány P. s. 1/c. Hungary

³ BCAM - Basque Center for Applied Mathematics
Alameda Mazarredo, 14, E - 48009 Bilbao
Basque Country, Spain

⁴ CAE Engineering Kft.
H-1122, Budapest, Ráth György u. 28. Hungary

e-mail: faragois@cs.elte.hu, izsakf@cs.elte.hu, tszabo@cs.elte.hu

Abstract

An implicit-explicit (IMEX) method is combined with some so-called Richardson extrapolation (RiEx) methods for the numerical solution of reaction-diffusion equations with pure Neumann boundary conditions. The results are applied to a model for determining the overpotential in a Proton Exchange Membrane (PEM) fuel cell.

1 Introduction

The numerical solution of advection-reaction-diffusion equations is a central problem in the numerical analysis. In practice, many important meteorological phenomena are modelled using reaction-diffusion equations (which are often supplemented with advection terms). Therefore,

* The first author was supported by Hungarian National Research Fund OTKA No. K67819.

†The first, second and the third author was supported by the European Union and co-financed by the European Social Fund (grant agreement no. TAMOP 4.2.1./B-09/1/KMR-2010-0003).

‡The Financial support of the National Office of Research and Technology (OMFB-00121-00123/2008) is acknowledged by the authors. The support of the project MTM2011-24766 (Spain) is also acknowledged.

the efficient numerical solution of these equations is of central importance. The numerical treatment of the boundary layer effect and the possibly stiff terms lead to challenging problems. The importance of this topic lies in the applicability of the corresponding models in the natural sciences including atmospheric modeling.

A previously [2] presented implicit-explicit (IMEX) method of second order in space is supplemented with Richardson extrapolation methods (passive and active) in time. The new method is developed for the numerical solution of reaction-diffusion equations with pure Neumann boundary conditions in order to have a method of second order both in space and in time. Richardson extrapolation is a very efficient method to increase the accuracy of many numerical methods. It consists of applying a given numerical scheme with different discretization parameters (in our case different time steps) and combining the obtained results with properly chosen weights [11].

2 Motivation

The method which we start from is stable under very mild conditions. If we can enhance also its time accuracy, we can have an efficient algorithm. In the atmospheric modeling it is particularly useful, since a fast method leading to an up-to-date forecast needs relatively large time steps. At the same time, in real life situations we have to run the corresponding simulations over many time steps, so the stability of the method is of primary importance.

To get a complex one-dimensional reaction-diffusion problem we cite here an interesting electrochemical model. Nowadays, electrical energy is the cleanest and most versatile energy that can be used in almost all fields of life. Due to the technical improvements, the utilization and the efficiency of producing electrical energy are increasingly growing.

In this section we compute numerically the overpotential in PEM fuel cells. These kinds of fuel cells “burn” hydrogen fuel and oxygen to water, producing electrical energy at a high efficiency without air pollution. Their operation can be reversible: they can also convert electrical energy into chemical energy.

The electro-chemical reactions take place at the anode and at the cathode on the boundary of two phases (solid and solution phase), while the charge neutrality is macroscopically preserved. Complex models [10] are needed to solve different phenomenological equations such as the Nernst-Planck equation for multiple mass transport, the Stefan-Maxwell equation for heat transfer, Ohm’s law for ionic migration and electron conductivity, and the equations of electrochemical kinetics. These models are usually solved by using only a single solver, e.g., Runge-Kutta, Newton or Crank-Nicholson methods.

Subramanian et al. [9] developed a method to reduce the number of the governing equations of Li-ion battery simulation by using different mathematical techniques. The original problem

with a proper discretization has 4800 equations which can be reduced to 49, and finally the simulation time of the discharge curve can be cut to 85 ms. However, in this model the double-layer capacitance was not included.

We focus here only on the evolution of the overpotential and we take into consideration both the inhomogeneity of the conducting media and the presence of the different phases in the cell. We perform the computations with realistic parameters.

2.1 Physical laws: homogeneous and heterogeneous models

In practice a consumer (some kind of electric device) is inserted into an electrical circuit, which is fed by the fuel cell. We assume that the current in the outer circuit is known ($I(t)$) and we can control it. The aim of the following investigation is to calculate the corresponding voltage, which is called the cell potential. This gives also the electric energy provided by the fuel cell, which is very important in the course of evaluating the performance of a fuel cell.

According to Kirchoff's law, the cell potential E_{cell} can be calculated by the following equation, see also [6]:

$$E_{cell}(t) = E_{OC}(t) - \eta^a(t) - \frac{W_{mem}}{\kappa_{mem}} I(t) - V^*(t), \quad (1)$$

where $t \in (0, T)$ denotes time. Here $E_{OC}(t) \approx 1.23 \text{ V}$ denotes the open circuit potential, which is present between the anode and cathode without the presence of any consumer.

Considering the simplest form of Ohm's law, the term $\frac{W_{mem}}{\kappa_{mem}} I(t)$ means the potential loss at the membrane, the thickness and conductivity of which are denoted by W_{mem} and κ_{mem} , respectively.

The calculation of the last quantity on the right-hand side (V^*), which refers to the potential loss at the cathode, needs a detailed analysis. The interval $(0, L)$ refers to the thickness of the cathode, where two phases are distinguished:

- The solution phase, where the hydrogen ions are conducted according to the rate κ_{eff} . The potential and the current density in this phase are denoted by ϕ_2 and i_2 , respectively.
- In the solid phase of the cathode electrons are conducted according to the rate σ_{eff} . The potential and the current density here are denoted by ϕ_1 and i_1 , respectively.

All of these quantities could be allowed to depend on time and space corresponding to the given assumptions and the structure of the fuel cell and the time evolution of the process.

Using the defined quantities, V^* in (Hiba! A hivatkozási forrás nem található.) can be given as

$$V^*(t) = \phi_1(t, L) - \phi_2(t, 0), \quad t \in (0, T). \quad (2)$$

The quantity we investigate in the governing equations is the overpotential

$$\eta(t, x) = \phi_1(t, x) - \phi_2(t, x) \geq 0, \quad x \in (0, L), \quad t \in (0, T). \quad (3)$$

In the calculation of the potentials, we choose the reference level to be at the left end of the solution phase, i.e., we define $\phi_2(t, 0) = 0$. This is in a good accordance with the uniqueness of the solutions in the corresponding equations. As we will see, the governing equations depend only on the spatial derivatives of the potentials, such that the above assumption is necessary to determine both $\phi_2(t, x)$ and $\eta_2(t, x)$. Then an immediate consequence of (2) and (3) is that

$$V^*(t) = \phi_1(t, L) = \eta(t, L) + \phi_2(t, L). \quad (4)$$

Applying Ohm's law for both phases we obtain

$$\begin{aligned} i_1(t, x) &= -\sigma_{eff}(x) \partial_x \phi_1(t, x) \\ i_2(t, x) &= -\kappa_{eff}(x) \partial_x \phi_2(t, x) \end{aligned} \quad (5)$$

and the principle of electroneutrality gives

$$-\partial_x i_1(t, x) = \partial_x i_2(t, x). \quad (6)$$

The conservation law for the currents (see [7]) results in the formula

$$\partial_x \left(\kappa_{eff}(x) \partial_x \phi_2(t, x) \right) = -a(x) C_{dl}(x) \partial_t \eta(t, x) - a(x) i_0(x) g \left(\alpha \frac{F}{RT} \eta(t, x) \right). \quad (7)$$

Here, the function $C_{dl}(x)$ gives the double-layer capacitance at the cathode side, and the last term yields the faradic current with $i_0(x)$, the exchange current density at the cathode. For the notations of the material coefficients we refer to the Appendix. The function $g : \mathbb{R} \rightarrow \mathbb{R}$ refers to the kinetics of the oxygen reduction reaction here. This should be an increasing function with $g(0) = 0$.

Remark 2.1 *Among the several approaches for the sake of simplicity we apply linear kinetics and, accordingly, we use*

$$g_L(u) = c(x)u, \quad (8)$$

where $c(x)$ is a given bounded non-negative function. Other possible choices are the following, which are going to be used in the course of the analysis and the numerical experiments [5].

- *Butler–Volmer kinetics:*

$$g_{BV}(u) = c(x)(\exp(u) - \exp(-u)). \quad (9)$$

- *diffusion kinetics:*

$$g_D(u) = j_D(x) \left(\frac{c(x) \exp(u)}{c(x)(\exp(u) + j_D(x))} - \frac{c(x) \exp(-u)}{c(x) \exp(-u) + j_D(x)} \right), \quad (10)$$

where $j_D(x)$ is the limiting current, which in this equation is acting as a diffusion coefficient. This choice provides the most accurate model of the cathode reaction.

In what follows the notation $g(u)$ stands for any of the above functions (g_L, g_{BV}, g_D).

At the left end of the cathode only the protons can exit to the membrane and similarly, at the right end (at the current collector), only the electrons can leave the cathode. Therefore $\partial_x \phi_1(t, 0) = 0$ and $\partial_x \phi_2(t, L) = 0$ such that using (3) we have the following boundary conditions

$$\begin{aligned} \partial_x \eta(t, 0) = -\partial_x \phi_2(t, 0) &= -\frac{1}{\kappa_{eff}(0)} I(t), \quad t \in (0, t_{max}), \\ \partial_x \eta(t, L) = \partial_x \phi_1(t, L) &= \frac{1}{\sigma_{eff}(L)} I(t), \quad t \in (0, t_{max}). \end{aligned} \quad (11)$$

Although we have listed all physical principles and the governing equations here, the corresponding equations are not yet ready for the solution, since (7) contains also the unknown term $\phi_2(t, x)$.

2.2 Governing equations in the heterogeneous case

In this section we will obtain an explicit equation for the overpotential $\eta(t, x)$ by eliminating the term $\phi_2(t, x)$ in (7) without assuming constant material and kinetic coefficients.

The physical laws in (5), (6), (7) and (11) can be rewritten into a single reaction-diffusion equation of type (21) for the unknown function η :

$$\begin{aligned} aC_{dl} \partial_t \eta(t, x) &= \partial_x \left(\frac{\kappa_{eff}}{\kappa_{eff} + \sigma_{eff}} \right) \left(-I(t) + \sigma_{eff} \partial_x \eta(t, x) \right) \\ &+ \frac{\kappa_{eff}}{\kappa_{eff} + \sigma_{eff}} \partial_x \left(\sigma_{eff} \partial_x \eta(t, x) \right) - ai_0 g \left(\alpha \frac{F}{RT} \eta(t, x) \right) \\ &= \partial_x \left[\frac{\kappa_{eff} \sigma_{eff}}{\kappa_{eff} + \sigma_{eff}} \partial_x \eta(t, x) \right] - \partial_x \left(\frac{\kappa_{eff}}{\kappa_{eff} + \sigma_{eff}} \right) I(t) \end{aligned}$$

$$-ai_0 g \left(\alpha \frac{F}{RT} \eta(t, x) \right) \quad (12)$$

For the corresponding initial-boundary value problem we use the initial value

$$\eta(0, x) = 0, \quad x \in (0, L), \quad (13)$$

and (12) is equipped with the Neumann type boundary conditions in (11). \square

Remark: We can express $\phi_2(t, x)$ as

$$\partial_x \phi_2(t, x) = \frac{1}{\kappa_{eff}(x) + \sigma_{eff}(x)} \left(I(t) - \sigma_{eff}(x) \partial_x \eta(t, x) \right), \quad (14)$$

and consequently, by the assumption $\phi_2(t, 0) = 0$ (see the explanation after (3)) we have

$$\phi_2(t, x) = \int_0^x \left(-\frac{\sigma_{eff}(t, s)}{\kappa_{eff}(t, s) + \sigma_{eff}(t, s)} \partial_s \eta(t, s) + \frac{1}{\kappa_{eff}(t, s) + \sigma_{eff}(t, s)} I(t) \right) ds. \quad (15)$$

Therefore, according to (4) we can give the potential loss V^* at the anode as

$$\begin{aligned} V^*(t) &= \eta(t, L) + \phi_2(t, L) \\ &= \eta(t, L) + \int_0^L -\frac{\sigma_{eff}(t, s)}{\kappa_{eff}(t, s) + \sigma_{eff}(t, s)} \partial_s \eta(t, s) + \frac{1}{\kappa_{eff}(t, s) + \sigma_{eff}(t, s)} I(t) ds. \end{aligned} \quad (16)$$

This completes the computation of the right-hand side of (**Hiba! A hivatkozási forrás nem található.**), and the desired quantity $E_{cell}(t)$ can be given.

Remark: According to the notations of the second section of this work we have that

$$p = \frac{1}{aC_{dl}}, \quad q = \frac{\kappa_{eff}\sigma_{eff}}{\kappa_{eff} + \sigma_{eff}} \quad \text{and} \quad F(t, x, \eta(t, x)) = -\frac{i_0}{C_{dl}} g \left(\alpha \frac{F}{RT} \eta(t, x) \right) - \frac{1}{aC_{dl}} \partial_x \left(\frac{\kappa_{eff}}{\kappa_{eff} + \sigma_{eff}} \right) I(t) \quad (17)$$

2.3 Model problem

For testing the method in the article, we investigate here a model problem. Based on real measurements we have

$\kappa_{eff} \approx 0.002$ and $\sigma_{eff} \approx 1.8$ and accordingly, we define

$$\kappa_{eff}(t, x) \approx 0.002 - 0.001x \quad \text{and} \quad \sigma_{eff}(t, x) \approx 1.8 + 0.001x. \quad (18)$$

Consequently,

$$\kappa_{eff} + \sigma_{eff} = 1.801 \text{ and } \frac{\kappa_{eff}}{\sigma_{eff} + \kappa_{eff}}(t, x) = \frac{2-x}{1801}.$$

For simplicity, we did not incorporate time dependence yet, but our analysis extends also to the case of time dependent conductivity parameters. If the analytic solution of the governing equation (12) is

$$\eta(t, x) = \frac{t^2}{4} \cdot \left(1 + \left(x - \frac{1801}{1803}\right)^2\right), \quad (19)$$

we can verify that the equalities

$$\begin{aligned} -\frac{1}{\kappa_{eff}(t,0)} I(t) &= \partial_x \eta(t, 0) = \frac{t^2}{2} \frac{1801}{1803} \\ \frac{1}{\sigma_{eff}(t,1)} I(t) &= \partial_x \eta(t, 1) = -\frac{t^2}{2} \left(1 - \frac{1801}{1803}\right) \end{aligned} \quad (20)$$

hold true such that $\partial_x \eta(t, 0)$ and $\partial_x \eta(t, 1)$ correspond to u_l and u_r in (21), where $I(t) = 10^{-3} \cdot \frac{1801}{1803} t^2$. These show that the boundary conditions in (11) are satisfied.

Using all parameters we can give $C_{dl}(x)$ such that η in (19) is the solution of (12) with the boundary conditions in (11).

It is justified to use the numerical method in Section 4 to approximate u since the Assumptions , and are satisfied:

- According to (17) and the choice of the linear kinetics,

$$\partial_3 F(t, x, u) = c(x) \alpha \frac{F}{RT},$$

which is bounded.

- The coefficient functions p and q given in (17) are obviously positive.
- The inequalities in Assumption have been verified consecutively in the time steps during the simulations. These results are shown in Figure 1. One can see that using a reasonably accurate space discretization we can simulate the underlying process over sufficiently long time.

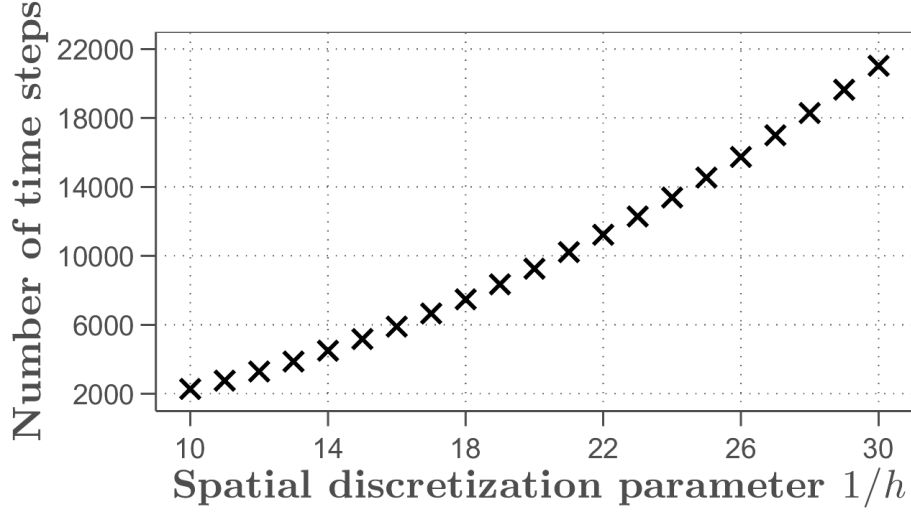


Figure 1: Number of steps N with step length $\tau = 1$ s until Assumption is satisfied vs. the number n of the grid points on the interval $I = 1$ cm.

3 Finite Difference Approximation

We use the following reaction-diffusion equation as a prototype to investigate some finite difference approximation:

$$\begin{cases} \partial_t u(t, x) = p(t, x) \partial_x (q(t, x) \partial_x u(t, x)) + F(t, x, u(t, x)), & t \in (0, T), \quad x \in I \\ u(0, x) = u_0(x), & x \in I \\ \partial_x u(t, h_l) = u_l(t), \quad \partial_x u(t, h_r) = u_r(t), & t \in (0, T), \end{cases} \quad (21)$$

for the unknown function u on the interval $I = (h_l, h_r) \subset \mathbb{R}$ over the time domain $[0, T)$, where the coefficient functions $p, q \in C^1([0, T] \times I)$, the reaction term $F \in C^1([0, T] \times I \times \mathbb{R})$ and the fluxes $u_l, u_r \in C^1[0, T]$ are given.

For the numerical approximation we use a staggered grid: I is divided into n uniform subintervals of length

$h = \frac{h_r - h_l}{n}$ such that

$$h_j := h_l + \frac{2j-1}{2|I|} h, \quad j = 1, 2, \dots, n \quad \text{and} \quad h_{j+\frac{1}{2}} := h_l + \frac{j}{|I|} h, \quad j = 0, 1, \dots, n$$

denote the midpoints and the endpoints of the subintervals, respectively as shown in the following figure:



For the time discretization we use the time step $\tau = \frac{T}{N}$ and the notation $t_k := \tau \cdot k$.

We denote the vector of unknowns by

$$\mathbf{u}^k = (u_1^k, u_2^k, \dots, u_n^k),$$

where $u_j^k \approx u(t_k, h_j)$. The values of the coefficient function $p_j^k = p(t_k, h_j)$ are defined in the midpoints of the subintervals, *i. e.*, $k = 0, 1, \dots, N$ and $j = 1, 2, \dots, n$. Accordingly, we use the notations

$$\mathbf{u}(k, \cdot) = (u(t_k, h_1), u(t_k, h_2), \dots, u(t_k, h_n))^T$$

and

$$\mathbf{F}(t_{k+1}, h, \mathbf{u}^k) = (F(t_{k+1}, h_1, u_1^k), \dots, F(t_{k+1}, h_n, u_n^k))^T.$$

At the same time the values of the coefficient function $q_{j+\frac{1}{2}}^k = q\left(t_k, h_{j+\frac{1}{2}}\right)$ are computed at the end points of the subintervals, *i. e.*, $k = 0, 1, \dots, N$ and $j = 0, 1, \dots, n$.

4 The IMEX scheme

We developed a finite difference scheme in [2]. To discuss the corresponding extrapolation method we summarize the notations and results in [2]. For the proof of the statements we refer to this work. We developed a finite difference scheme following the *method of lines*: the vector of unknowns at the $(k + 1)$ th time step is determined from that at the k th time step [2].

Using the notations in Section 3 we consider the following finite difference approximation of (21):

$$\left\{ \begin{array}{l}
u_j^0 = u_0(h_j), j = 1, 2, 3, \dots, n \\
\frac{u_j^{k+1} - u_j^k}{\tau} = \frac{1}{h} p_j^{k+1} \left(q_{j+\frac{1}{2}}^{k+1} \frac{u_{j+1}^{k+1} - u_j^{k+1}}{h} - q_{j-\frac{1}{2}}^{k+1} \frac{u_j^{k+1} - u_{j-1}^{k+1}}{h} \right) \\
+ F(t_{k+1}, h_j, u_j^k), k = 0, 1, \dots, N-1, j = 2, 3, \dots, n-1 \\
\frac{u_1^{k+1} - u_1^k}{\tau} = \frac{1}{h} p_1^{k+1} \left(q_{\frac{3}{2}}^{k+1} \left(\frac{u_2^{k+1} - u_1^{k+1}}{h} + \frac{\frac{3}{23}u_2^{k+1} - \frac{2}{23}u_1^{k+1} - \frac{1}{23}u_3^{k+1}}{h} - \frac{1}{23}u_l(t_{k+1}) \right) \right. \\
\left. - q_{\frac{1}{2}}^{k+1}u_l(t_{k+1}) \right) + F(t_{k+1}, h_1, u_1^k), k = 0, 1, \dots, N-1 \\
\frac{u_n^{k+1} - u_n^k}{\tau} = \frac{1}{h} p_n^{k+1} \left(-q_{n-\frac{1}{2}}^{k+1} \left(\frac{u_n^{k+1} - u_{n-1}^{k+1}}{h} - \frac{\frac{3}{23}u_{n-1}^{k+1} - \frac{1}{23}u_{n-2}^{k+1} - \frac{2}{23}u_n^{k+1}}{h} - \frac{1}{23}u_r(t_{k+1}) \right) \right. \\
\left. + q_{n+\frac{1}{2}}^{k+1}u_r(t_{k+1}) \right) + F(t_{k+1}, n, u_n^k), k = 0, 1, \dots, N-1
\end{array} \right. \quad (22)$$

Under the following assumptions the consistency (of second order) and the convergence are proven in our previous work [2]

Assumption 1 $\partial_3 F : \mathbb{R}^3 \rightarrow \mathbb{R}$ is bounded; $\partial_3 F \leq F_{max} \in \mathbb{R}$.

Note that a similar assumption is usual in the literature, see, e.g., [3], [4].

Assumption 2 The coefficient functions p and q are nonnegative.

Assumption 3 For all $k = 1, 2, \dots, N$ the following inequalities hold true:

$$s_1^k = \frac{25}{23}d_1^k - \frac{1}{23}\frac{d_1^k}{d_2^k} - \frac{1}{23}\frac{d_1^k c_2^k}{d_2^k} > 0$$

$$s_2^k = \frac{25}{23}c_n^k - \frac{1}{23}\frac{c_n^k}{c_{n-1}^k} - \frac{1}{23}\frac{c_n^k d_{n-1}^k}{c_{n-1}^k} > 0.$$

Remark: The inequalities in assumption are equivalent with

$$25d_2^k > 1 + c_2^k \Leftrightarrow rp_2 \left(25q_{\frac{5}{2}} - q_{\frac{3}{2}} \right) > 1$$

(23)

$$25c_{n-1}^k > 1 + d_{n-1}^k \Leftrightarrow rp_{n-1} \left(25q_{n-\frac{1}{2}} - q_{n+\frac{1}{2}} \right) > 1$$

Lemma 4.1 *The scheme (22) is consistent with the boundary value problem (21), and the corresponding order of consistency is $\mathcal{O}(\tau) + \mathcal{O}(h^2)$.*

To rewrite (22) into a more accessible form we introduce the notations for $j = 1, 2, \dots, n$:

$$rp_j^k q_{j-\frac{1}{2}}^k = c_j^k \text{ and } rp_j^k q_{j+\frac{1}{2}}^k = d_j^k \text{ with } r = \frac{\tau}{h^2}.$$

With these we define the matrix

$$\begin{pmatrix} 1 + \frac{25}{23}d_1^k & -\frac{26}{23}d_1^k & \frac{1}{23}d_1^k & & 0 & \dots & 0 \\ -c_2^k & 1 + c_2^k + d_2^k & -d_2^k & & 0 & \dots & 0 \\ & 0 & -c_3^k & 1 + c_3^k + d_3^k & -d_3^k & \ddots & 0 \\ & \vdots & \vdots & \vdots & \vdots & 1 + c_{n-1}^k + d_{n-1}^k & -d_{n-1}^k \\ 0 & \dots & 0 & 0 & -c_{n-1}^k & \frac{26}{23}c_n^k & 1 + \frac{25}{23}c_n^k \\ 0 & \dots & 0 & \frac{1}{23}c_n^k & -\frac{26}{23}c_n^k & & 1 + \frac{25}{23}c_n^k \end{pmatrix}$$

and the vector

$$\mathbf{v}^k = \left(\frac{\tau}{h} p_1^k \left(q_{\frac{3}{2}}^k \cdot \frac{1}{23} \cdot u_l(t_k) + q_{\frac{1}{2}}^k u_l(t_k) \right), 0, \dots, 0, -\frac{\tau}{h} p_n^k \left(q_{n-\frac{1}{2}}^k \cdot \frac{1}{23} \cdot u_r(t_k) + q_{n+\frac{1}{2}}^k u_r(t_k) \right) \right)^T.$$

The time stepping in (22) then can be given as

$$\mathbf{u}^k = A_{k+1,h} \mathbf{u}^{k+1} - \tau \mathbf{F}(t, h, \mathbf{u}^k) + \mathbf{v}^{k+1}. \quad (24)$$

The following property of $A_{k,h}$ is of central importance.

Lemma 4.2 *For all $h > 0$ and $k = 0, 1, \dots, N$ we have $\|A_{k,h}^{-1}\|_{\infty} = 1$.*

Theorem 4.1 [2] *The finite difference method given by (22) converges to the solution of (21) and*

$$\max_{j \in \{1,2,\dots,n\}} \|u_j^N - u(T, h_j)\| = \mathcal{O}(\tau) + \mathcal{O}(h^2). \quad (25)$$

Proof: The error of the solution in the consecutive time steps is defined as

$$(e_1^k, e_2^k, \dots, e_n^k) = \mathbf{e}^k = u(k, \cdot) - \mathbf{u}^k.$$

The consistency of the scheme implies that

$$\mathbf{u}(k, \cdot) = A_{k+1, h} \mathbf{u}(k+1, \cdot) - \tau \mathbf{F}(t, h, \mathbf{u}(k, \cdot)) + \mathbf{v}_{k+1} - \mathcal{R}^k,$$

where

$$\|\mathcal{R}^k\|_\infty = \tau(\mathcal{O}(\tau) + \mathcal{O}(h^2)). \quad (26)$$

This together with (24) gives that

$$e^k = A_{k+1, h} e^{k+1} - \tau \left(\mathbf{F}(t, h, \mathbf{u}^k) - \mathbf{F}(t, h, \mathbf{u}(k, \cdot)) \right) + \mathcal{R}^k$$

or in an equivalent form

$$\mathbf{u}^k - \mathbf{u}(k, \cdot) = e^{k+1} = A_{k+1, h}^{-1} e^k + \tau A_{k+1, h}^{-1} \left(\mathbf{F}(t, h, \mathbf{u}^k) - \mathbf{F}(t, h, \mathbf{u}(k, \cdot)) \right) + \mathcal{R}^{k+1}.$$

Therefore, using the result in Lemma , the Lagrange inequality and Assumption we obtain

$$\|e^{k+1}\|_\infty \leq \|e^k\|_\infty + \tau \mathbf{F}_{max} \|e^k\|_\infty + \|\mathcal{R}^{k+1}\|_\infty \quad (27)$$

for all $k = 1, 2, \dots, N$. The consecutive application of (27) gives that

$$\begin{aligned} \|e^N\|_\infty &\leq (1 + \tau \mathbf{F}_{max})^{N-1} \|\mathcal{R}^1\|_\infty + (1 + \tau \mathbf{F}_{max})^{N-2} \|\mathcal{R}^2\|_\infty + \dots + \|\mathcal{R}^N\|_\infty \\ &\leq N(1 + \tau \mathbf{F}_{max})^N \max_{j \in \{1, 2, \dots, n\}} \|\mathcal{R}^j\|_\infty \leq T e^{T \cdot \mathbf{F}_{max}} \frac{\max_{j \in \{1, 2, \dots, n\}} \|\mathcal{R}^j\|_\infty}{\tau} \end{aligned}$$

such that according to (26) we obtain the estimate in the theorem. \square

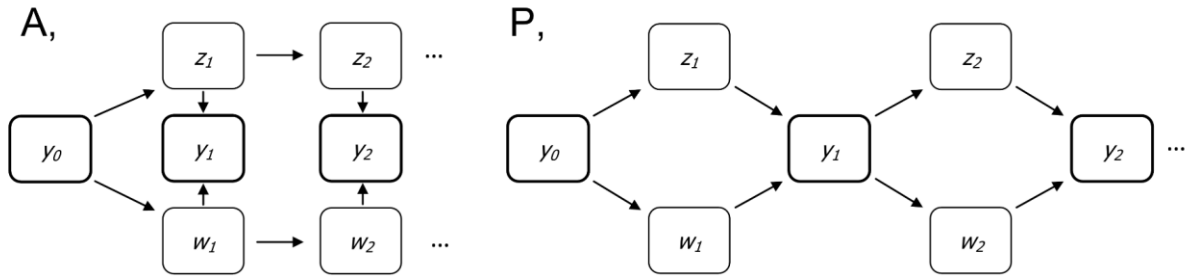


Figure 2: Schematic comparison of the different Richardson extrapolation procedures: passive method (left) and active method (right)

5 Richardson extrapolation

According to Theorem 3, the previously presented numerical scheme provides us 2nd order of consistency in space, but not in time. We apply the Richardson extrapolation as a powerful device to increase the accuracy of the numerical method in [2]. In general, it consists of the application of the given numerical scheme. In order to have a 2nd order scheme both in space and in time, the application of an other mathematical device is crucial.

Richardson extrapolation is a powerful device to increase the accuracy of some numerical method. It consists in applying the given numerical scheme with different discretization parameters (in our case, Δt and $\Delta t/2$) and combining the obtained numerical solutions by properly chosen weights. Namely, if p denotes the order of the chosen numerical method, w_n the numerical solution obtained by $\Delta t/2$ and z_n that obtained by Δt , then the combined solution

$$y_n = \frac{2^p w_n - z_n}{2^p - 1}$$

has an accuracy of order $p + 1$. This method was first used by L. F. Richardson [8], who called it "the deferred approach to the limit". The Richardson extrapolation is especially widely used for time integration schemes, where, as a rule, the results obtained by two different time-step sizes are combined.

The Richardson extrapolation can be implemented in two different ways when one attempts to increase the accuracy of a time integration method (see Figure 2), namely, passive and active Richardson extrapolations [11]. These two versions of the Richardson extrapolation are also described in [1], where they are called global and local Richardson extrapolations. The main difference between these two methods is that in the case of passive extrapolation the numerical solutions obtained with different step sizes are computed independently of the result of the extrapolation obtained at the previous time step, while in the active version the result of the extrapolation is used as initial condition in each time step.

Remark 5.1 *It is not difficult to see that if the passive device is applied and the underlying method has some qualitative properties, then the combined method also possesses this property. However, if the active device is used, then this is not valid anymore: any property of the underlying method does not imply the same property of the combined method. Therefore, the active Richardson extrapolation requires further investigation when a given numerical method is applied.*

6 Numerical results

We present some numerical results here corresponding to the model problem discussed in Section 2.3. The analytic and the numerical solution are compared at $T = 1$ in Figure 3 for a single parameter set.

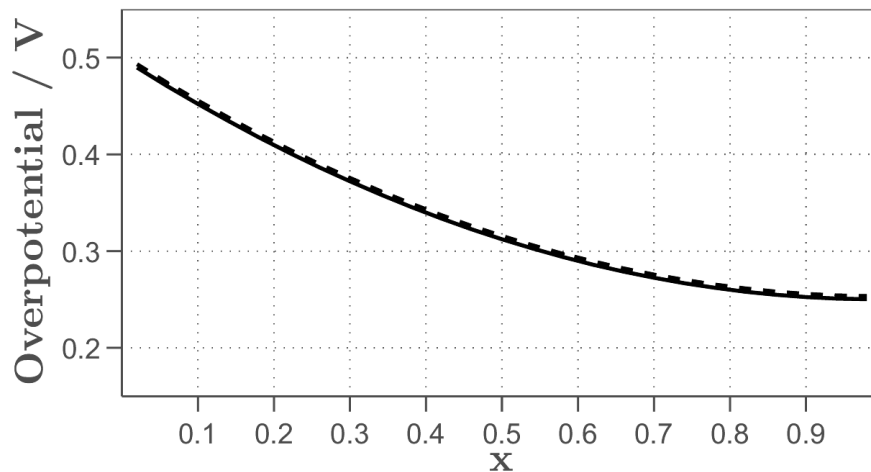


Figure 3: Analytic solution (19) of (12) (continuous line) and the numerical approximation (dashed line) obtained by the method in (22) with $T = 1$, $N = 25$ and $\tau = 0.01$ for the test problem in Section 2.3. The remaining parameters are given in the Appendix.

We investigated the order of convergence in the $\|\cdot\|_\infty$ norm experimentally with respect to the spatial discretization. To this aim we consecutively refined the grid and the time step simultaneously such that the ratio $\frac{\tau}{h^2}$ is kept at constant level. Accordingly, in the figures we only investigate the dependence of the $\|\cdot\|_\infty$ -norm error on the number $\frac{1}{h}$ of the spatial grid points. The corresponding results are shown in Figure 4. The numerical results confirm our expectation in Section 4: we can fit accurately a line of slope -2 to the log-log data, which shows a second order convergence with respect to the spatial discretization parameter, see Figure 4.

In Figure 5 we illustrated the order of the convergence of the numerical models obtained by the application of the two types of Richardson extrapolation (active and passive) methods. Comparing this result to Figure 4. (i.e. to the results obtained without Richardson extrapolation) one can easily see that the application of these methods led to lower approximation errors. Though in the case of active Richardson extrapolation, the convergence becomes second order only in the limit $h \rightarrow 0$.

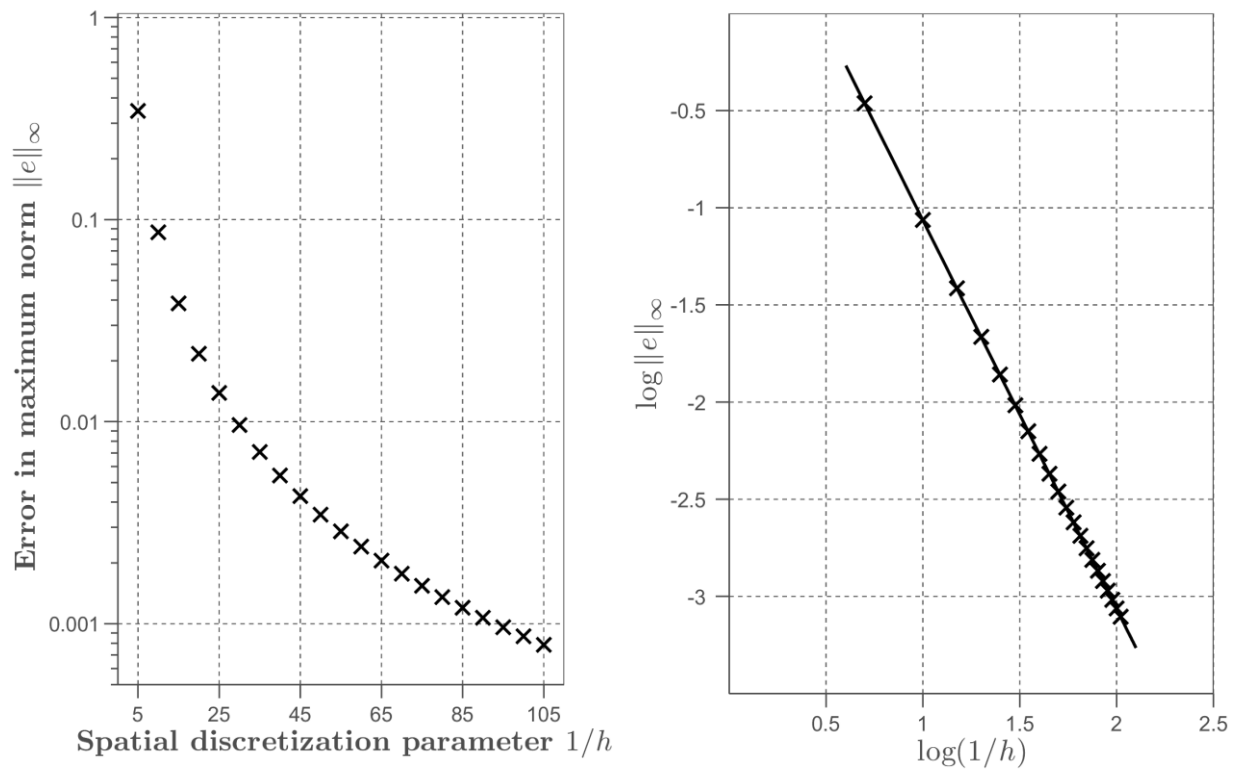


Figure 4: $\|\cdot\|_\infty$ norm error in the numerical solution (obtained by the presented IMEX method) for the test problem in Section 2.3 vs. the spatial discretization parameter (left). Log-log plot of the error vs. the spatial discretization parameter and a fitted line with slope -2 (right).

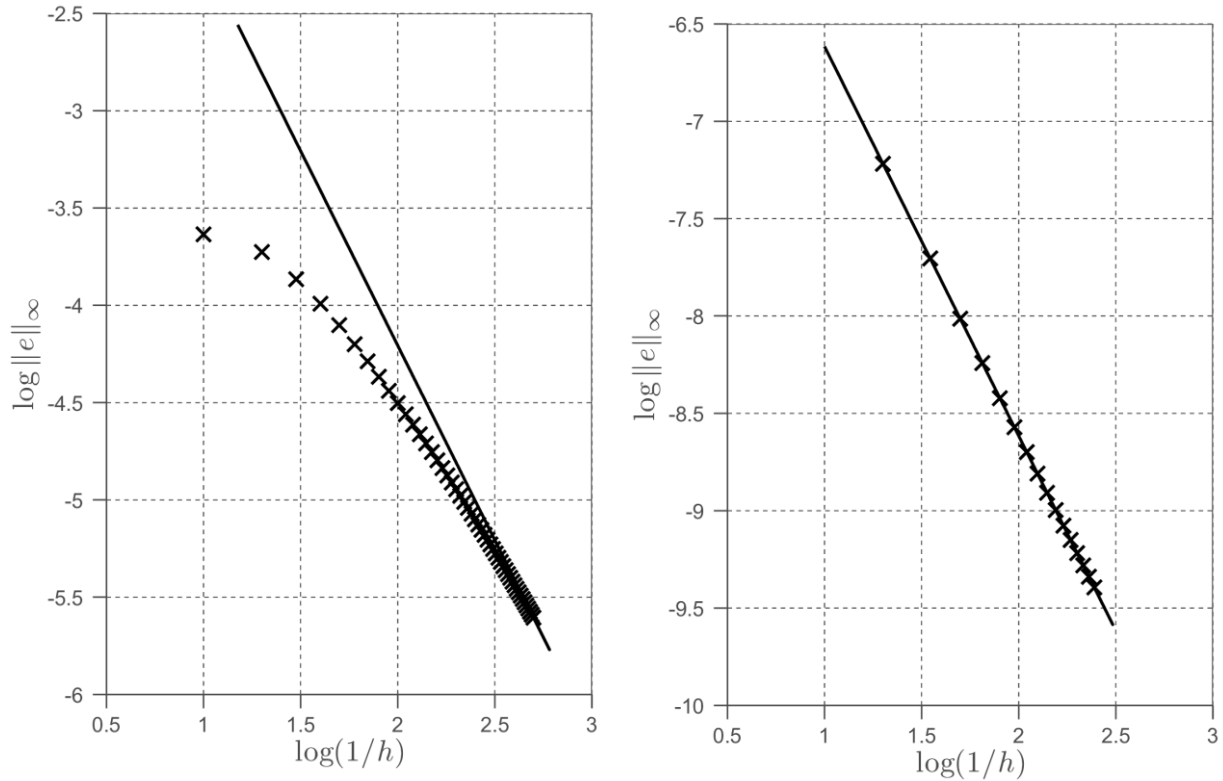


Figure 5: Log-log plot of the $\|\cdot\|_\infty$ norm error vs. the spatial discretization parameter for the active Richardson extrapolation (left) and the passive Richardson extrapolation (right).

7 Conclusions

Our results have proven that the combination of the presented implicit-explicit method with some Richardson extrapolation methods can be a useful device for solving reaction-diffusion equations numerically. The numerical results in the previous section are also supporting our theoretical analysis.

8 Appendix

Symbol	Description	Unit
a	Specific interfacial area	cm^{-1}
C_{dl}	Double-layer capacitance	F/cm^2
E_{cell}	Cell potential	V
E_{OC}	Open circuit potential	V
F	Faraday constant (96487)	C/mol
I	Total cell current density	A/cm^2
i_0	Exchange current density at the cathode	A/cm^2
i_0^a	Exchange current density at the anode	A/cm^2
i_1	Solid phase current density at the cathode	A/cm^2
i_2	Solution phase current density at the cathode	A/cm^2
i_f	Faradaic current density	A/cm^3
j_D	Limiting current at the cathode	A/cm^2
L	Thickness of the cathode	cm
R	Universal gas constant (8.3144)	J/molK
T	Cell temperature	K
V^*	Potential loss at the cathode	V
W_{mem}	Membrane thickness	cm
α	Transfer coefficient in the cathode	
α_a^a	Anodic transfer coefficient at the anode	
α_c^a	Cathodic transfer coefficient at the anode	
η	Overpotential at the cathode	V
η^a	Overpotential at the anode	V
ν^2	Dimensionless Exchange current density	
ϕ_1	Solid phase potential	V
ϕ_2	Solution phase potential	V
κ_{eff}	Effective solution phase conductivity	S/cm
σ_{eff}	Effective solid phase conductivity	S/cm
σ_{mem}	Membrane conductivity	S/cm

References

- [1] M. A. Botchev and J. G. Verwer. Numerical integration of damped Maxwell equations. *SIAM J. Scientific Computing*, 31(2):1322–1346, 2009.
- [2] I. Faragó, F. Izsák, T. Szabó, and A. Kriston. An IMEX scheme for reaction-diffusion equations: application for a PEM fuel cell model., *Cent. Eur. J. Math.* 11(4), 746-759, 2013.
- [3] D. Hoff. Stability and convergence of finite difference methods for systems of nonlinear reaction-diffusion equations. *SIAM J. Numer. Anal.*, 15(6):1161–1177, 1978.
- [4] T. Koto. IMEX Runge-Kutta schemes for reaction-diffusion equations. *J. Comput. Appl. Math.*, 215(1):182–195, 2008.
- [5] A. Kriston, G. Inzelt, I. Faragó, and T. Szabó. Simulation of the transient behavior of fuel cells by using operator splitting techniques for real-time applications. *Computers and Chemical Engineering*, 34(3):339–348, 2010.
- [6] S. Litster and N. Djilali. Mathematical modelling of ambient air-breathing fuel cells for portable devices. *Electrochimica Acta*, 52(11):3849–3862, 2007.
- [7] J. Newman and K. E. Thomas-Alyea. *Electrochemical systems*. John Wiley & Sons, Inc., Hoboken, New Jersey, third edition, 2004.
- [8] L. F. Richardson. The deferred approach to the limit, i-single lattice. *Philosophical Transactions of the Royal Society of London*, 226:299–349, 1927.
- [9] V. R. Subramanian, V. Boovaragavan, and V. D. Diwakar. Toward real-time simulation of physics based lithium-ion battery models. *Electrochemical and Solid-State Letters*, 10(11):A255–A260, 2007.
- [10] C. Ziegler, H. M. Yu, and J. O. Schumacher. Two-phase dynamic modeling of pemfcs and simulation of cyclo-voltammograms. *Journal of The Electrochemical Society*, 152(8):A1555–A1567, 2005.
- [11] Z. Zlatev, I. Faragó, and A. Havasi. Stability of the richardson extrapolation applied together with the Θ -method. *J. Comput. Appl. Math.*, 235(2):507–517, 2010.